Journal of Power Sources 196 (2011) 1855–1863

Contents lists available at ScienceDirect

Journal of Power Sources

journal homepage: www.elsevier.com/locate/jpowsour

A novel, effective and low cost catalyst for methanol oxidation based on nickel ions dispersed onto poly(*o*-toluidine)/Triton X-100 film at the surface of multi-walled carbon nanotube paste electrode

Jahan-Bakhsh Raoof*, Reza Ojani, Sayed Reza Hosseini

Electroanalytical Chemistry Research Laboratory, Department of Analytical Chemistry, Faculty of Chemistry, Mazandaran University, 3rd Kilometer of Air Force Road, Postal Code 47416-95447, Babolsar, Iran

ARTICLE INFO

Article history:
Received 4 July 2010
Received in revised form
19 September 2010
Accepted 21 September 2010
Available online 1 October 2010

Keywords:
Triton X-100
Poly(*o*-toluidine)
Methanol oxidation
Nickel(II) ions
Multi-walled carbon nanotube paste electrode

ABSTRACT

In this work, for the first time an aqueous solution of Triton X-100 (TX-100) [t-octyl phenoxy polyethoxy ethanol] non-ionic surfactant is used as an additive for electropolymerization of *o*-toluidine (OT) onto multi-walled carbon nanotube paste electrode (CNTPE), which is investigated as a novel matrix for dispersion of nickel ions. The growth of polymeric film in the absence of TX-100 is poor, while it considerably increases in the presence of the surfactant and its growth is continued up to 60th cycle. The as-prepared substrate is used as porous matrix for dispersion of transition metal ions of Ni(II) to POT/TX-100 film by immersing the modified electrode in a 0.1 M nickel sulfate solution. The electrochemical characterization of this modified electrode exhibits redox behavior of Ni(III)/Ni(II) couple. It has been shown that POT/TX-100 at the surface of CNTPE improves catalytic efficiency of the dispersed nickel ions toward methanol oxidation. Then, using a chronoamperometric method, the catalytic rate constant, k, for methanol oxidation is found to be 7.40×10^4 cm^3 mol^{-1} s^{-1}. At the end of this work, long-term stability of this modified electrode has been investigated.

1. Introduction

There is increasing interest in the electrooxidation of methanol because of the development of direct methanol fuel cells (DMFCs) as power sources for electronic devices. The DMFC is a promising future technology as an alternative to conventional energy-generating devices due to its higher energy conversion efficiency, low-to-zero pollutant emissions, ready availability of methanol fuel, ease in distribution, and high energy [1]. Despite many efforts devoted to the DMFC development, their still remain problems to be overcome in terms of efficiency and power density. One of the reasons is the relatively slow kinetics of the methanol oxidation reaction (MOR) at the anode, which leads to high over potentials [2]. Most of the works reported for oxidation of methanol in the literature deal with Pt and Pt-based alloys in acid medium [3–11]. However, the cost price and limited supply of Pt constitute a major barrier to the development of DMFCs [12]. Also, Pt-based electrodes generally become deactivated due to surface poisoning by the reaction intermediates, particularly CO molecules [13].

It is, therefore, of interest to investigate low cost non-noble metals for electrocatalysis of the MOR in alkaline medium. An alkaline solution is considered superior to an acid solution in respect of kinetics as well as material stability standpoints [13–15]. Compared to an acid solution, a much wider range of materials are stable in alkaline solutions and can be used as anodes for methanol oxidation. Recently, several electrodes based on non-noble metals/oxides have been investigated as anodes for the MOR in an alkaline medium [16–20]. Among non-noble metals, nickel is a versatile catalytic material due to its surface oxidation properties.

Conducting polymer matrices have been employed as catalyst support materials for the oxidation of small organic molecules in place of conventional support because when particle catalyst is dispersed in carbon black, a part of the active sites remains inaccessible to the reactant molecules [21,22]. However, metal ions dispersed into conducting polymer support, not only provide access to large number of catalytic sites, but also offer the possibilities of spent catalyst recovery. On the other hand, it should be noticed that the nature of working electrode substrate in electropreparation of polymeric film is very important because the properties of polymeric films depend on the working electrode material. The ease and fast preparation and obtaining a new reproducible surface, the low residual current, porous surface, and low cost of carbon paste are some advantages of carbon paste electrode (CPE) over all other solid electrodes [23,24]. Also, an important method to obtain electrocatalyst with high performance and low cost is to disperse these compounds onto the supporters such as carbon. Finding a suitable

* Corresponding author. Tel.: +98 112 5342392; fax: +98 112 5342350.
E-mail address: j.raoof@umz.ac.ir (J.-B. Raoof).

0378-7753/$ – see front matter © 2010 Elsevier B.V. All rights reserved.
doi:10.1016/j.jpowsour.2010.09.046

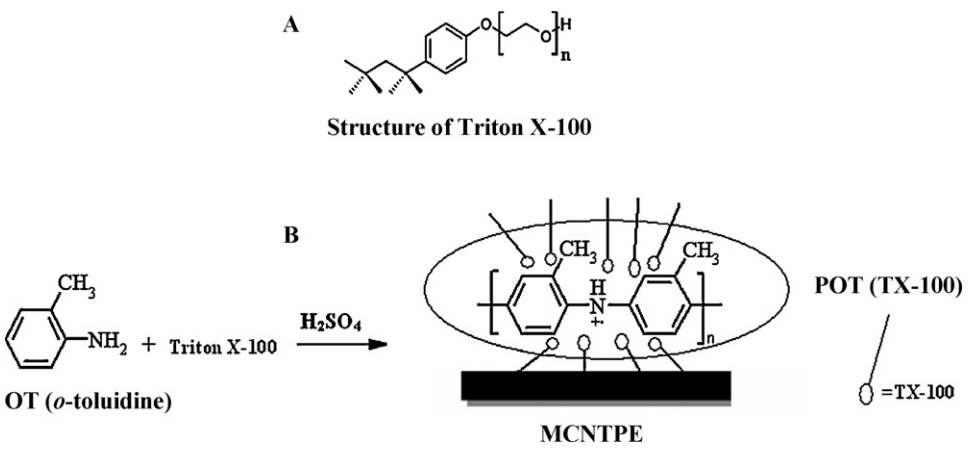

Scheme 1. (A) Structure of TX-100 non-ionic surfactant. (B) Proposed mechanism for the electropolymerization of *o*-toluidine in the presence of TX-100.

electrode material will be necessary for economic reasons. Carbon paste is a promising material for DMFC due to its advantages.

It has been seen that surfactants (surface active agents) play a very important role in electrode reactions, not only in solubilizing organic compounds, but also by providing specific orientation of the molecules at the electrode interface. These molecules can give rise to adsorbed layers of varying thickness monolayers, bilayers or multilayers of a very complex structure, thus affect the rate of electrode reaction. Surfactants affect the locus of polymerization and thus modify the molecular and supra-molecular structure and surface morphology of polymers. Most non-ionic surfactants are composed of a polyethylene oxide chain and hydrophobic part. These surfactants have been applied in many industrial and technological processes such as detergency, wetting, foaming, emulsification and lubrication [25]. On the other hand, non-ionic surfactants offer decreased sensitivity of the latex to acidity and ionic strength. Triton X-100 (Scheme 1A) is one of the non-ionic surfactants widely used in biochemical, chemical, industrial processes and in polarography as maximum suppressers.

Generally, studies involving use of the surfactant in electropreparation of novel conducting polymer support is rare. Recently, we have investigated the electrocatalysis of methanol oxidation based on nickel particles electrodeposited into poly(*m*-toluidine)-CTAB film on the carbon paste electrode [26]. The work was time consuming (15 min electrolysis at fixed potential) and CTAB can be only adsorbed on the electrode surface and changes the interfacial structure between electrode surface and electrolyte, which benefits the electropolymerization of MT. Our literature survey indicates that, there is no report about the electropolymerization of *o*-toluidine (OT) at the surface of multi-walled carbon nanotube paste electrode in the presence of TX-100 as an additive. The novelty of present work is due to the fact that unlike CTAB, TX-100 not only may be adsorbed on the electrode surface and alters the interfacial structure which facilitates the electropolymerization, but also acts as a dopant of the formed polymer film in parallel. CTAB with positive charge cannot act as a dopant during electropolymerization while TX-100 with oxygen atoms in head polar group can do it. Therefore, in this study, with respect to advantages of carbon nanotube (e.g., high accessible surface area, low resistance, and high stability), carbon paste and non-ionic surfactants, we have decided to investigate the effect of the surfactant on the electropolymerization and on growth of poly(*o*-toluidine) films. Therefore, poly(*o*-toluidine)/TX-100 modified CNTPE which is a new conductive organic matrix was prepared and allowed a better dispersion of nickel ions as a low cost electrocatalyst for electrocatalytic oxidation of methanol. This modified electrode can oxidize the methanol with high current density (over 18.5 mA cm^{-2}). Thus, this electrode can be a candidate in terms of high current density as an anode for power sources such as DMFCs.

2. Experimental

2.1. Materials

The solvent used in this work was double distilled water. Sulfuric acid (from Fluka) and sodium hydroxide (from Merck) were used as the supporting electrolytes. The $NiSO_4 \cdot 6H_2O$ (from Fluka), OT monomer and Triton X-100 (99%) from Merck were used as received. Methanol (from Merck) used in this work was analytical grade. High viscosity paraffin (density: 0.88 g cm^{-3}) (from Fluka) was used as the pasting liquid for CNTPE. Graphite powder (particle diameter: 0.10 mm, from Merck) and multi-walled carbon nanotube (with purity >95%, diameter 54 nm, length 1–10 μm, number of walls 3–15, from Nanostartech. Co., Tehran, Iran) were used as the working electrode substrates. The as-received multi-walled carbon nanotubes were treated with concentrated acids (H_2SO_4/HNO_3: 3/1) for purification and generation of oxygen functionalities on the surface of MWCNTs. All other reagents were of analytical grade.

2.2. Electrochemical measurement

Electrochemical experiments were performed using AUTOLAB PGSTAT 30 electrochemical analysis system and GPES 4.9 software package (Eco Chemie, Netherlands). The utilized three-electrode system was composed of a Ag|AgCl|KCl (3 M) as reference electrode, a platinum wire as auxiliary electrode, unmodified carbon paste and modified carbon nanotube paste as working electrode. All potentials reported in this article are referenced to the Ag|AgCl|KCl (3 M).

2.3. Electrode modification

A mixture of graphite powder (0.60 g) plus multi-walled carbon nanotubes (0.085 g) were blended by hand mixing with a mortar and pestle. Using a syringe, 0.40 g paraffin was added to the mixture and mixed well until a uniformly wetted paste is obtained. The resulting paste was then inserted in the bottom of a glass tube (internal radius: 1.7 mm). The electrical connection was implemented by a copper wire lead fitted into the glass tube. A fresh electrode surface was generated rapidly by extruding a small plug of the paste out of the tube and smoothing the resulting surface on white paper until a smooth shiny surface is observed. The unmodified carbon paste electrode was prepared in the same way without

adding carbon nanotubes to the mixture to be used for comparison purposes. Later modifications of the mentioned electrodes were performed in three steps:

(a) Electropolymerization of OT monomer by using potential cycling (10 cycles at a scan rate of potential, $\upsilon = 50\,mV\,s^{-1}$) between 0.0 and 1.2 V vs. Ag|AgCl|KCl (3 M) in aqueous solution containing 9.3 mM OT, 0.5 M H_2SO_4 and 5.0 mM of TX-100 for construction of POT (TX-100)/MCNTPE.
(b) Incorporation of Ni(II) ions (as inexpensive metallic ions) to the POT (TX-100) films by immersing the freshly electropolymerized CNTPE in a well-stirred aqueous 0.1 M $NiSO_4$ solution for accumulation time of 120 s.
(c) After nickel ions incorporation, the electrode was rinsed with distilled water. At beginning of experiments, the Ni/poly(*o*-toluidine)/TX-100 modified CNTPE (Ni/POT (TX-100)/MCNTPE) was immersed in 0.1 M NaOH solution and the potentials were cycled between 0.1 to 0.8 V at $\upsilon = 0.05\,V\,s^{-1}$ until a reproducible cyclic voltammogram was attained (10–15 cycles).

3. Results and discussion

3.1. Electrochemical polymerization

The poly(*o*-toluidine) film was prepared on the surface of carbon nanotube paste electrode in the absence and presence of TX-100. Fig. 1A shows the typical multi-sweep cyclic voltammograms during the electropolymerization of OT in the presence of TX-100. As can be seen in this figure, in the first anodic sweep, the oxidation of OT occurs as a distinct irreversible anodic peak ($E_p = 0.93$ V). Three redox peaks are observed for the polymerization of OT in H_2SO_4 solution [27–31]. A part of the oxidation products of OT is deposited on the electrode, as a poly(*o*-toluidine) film. The oxidation peak current of monomer is decreased with increasing of the number of potential cycles up to 4th cycle. The decreasing of oxidation current is due to the loss of activity of the electrode surface when covered with newly formed polymer film. In the presence of TX-100, the rate of polymerization is considerably increased. Furthermore, under successive potential cycling, the peak currents related to the polymer are significantly increased, and their growth continued up to 60th cycle. The surfactant tends to accumulate at the electrode|electrolyte interface and draws in the monomer, thereby enhancing the local concentration. These results show that, in the presence of TX-100, the monomers can easily reach toward the electrode surface and produce more monocation radicals. TX-100 improves the OT solubility and allows a well-defined polymer growth on the working electrode. Moreover, their polymers show a better stability than those obtained in the absence of TX-100. For comparison, Fig. 1B shows typical cyclic voltammograms during polymerization of OT in the absence of TX-100. Electrochemical signal of the conducting poly(*o*-toluidine) film prepared from the solution with TX-100 is greatly improved in comparison with that from the solution without the surfactant. The effect of the additive can be analyzed by looking into its molecular structure. The head group of TX-100 (PEO chains) is polar. TX-100 molecules may be adsorbed on the electrode surface and change the interface structure between the electrode and the electrolyte solution, which benefits the electropolymerization of this monomer. The proposed mechanism for the electrochemical polymerization of OT with TX-100 is shown in Scheme 1B. The oxygen atoms in the polyoxyethylene group of TX-100 may attract the positive charge of monomer radical, resulting in $OT^{\bullet+}$–TX-100 form. Therefore, TX-100 makes easier electropolymerization for OT. Indeed, the presence of TX-100 decreases the monomer oxidation potential and induces the polymerization.

3.2. Cyclic voltammetry behavior of the POT (TX-100)/MCNTPE

The stability of prepared films is checked with CV in 0.5 M H_2SO_4 solution, which shows decreasing in current at initial ten cycles and the current almost remains constant afterward. In the first cycle a shoulder is observed at potential redox around 0.48 V. The shoulder disappeared after repeatedly cycling the film in TX-100 free sulfuric acid solution. This redox peak in the cyclic voltammograms is due to adsorption of quinone and/or hydroquinone, generated during the growth of polymer film, which is strongly adsorbed in the polymer matrix [27]. For comparison, cyclic voltammetry behaviors of POT/MCNTPE and POT (TX-100)/MCNTPE are shown in Fig. 2. The electrodes demonstrate their electrochemical activities, which are characterized by typical oxidation and reduction responses. Poly(*o*-toluidine)/TX-100 films have considerably higher redox current than the normal poly(*o*-toluidine) film. The difference in redox currents reflect the effective active surface areas that are accessible to the electrolytes at POT (TX-100)/MCNTPE. Apparently, the porous POT (TX-100) films have higher effective surface areas. This improvement of doping–undoping rate results from the increase of surface area and porous structure, which are of benefit to the ion diffusion and migration [32]. Furthermore, the POT (TX-100)

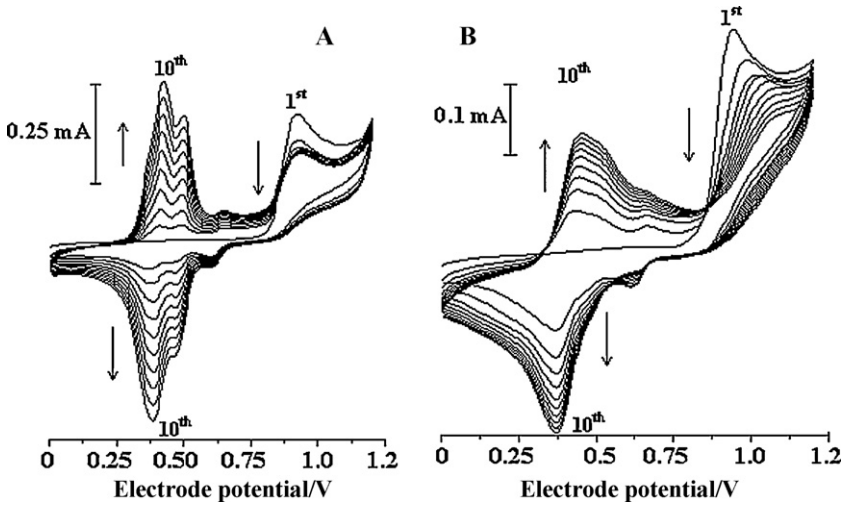

Fig. 1. Electropolymerization of OT in a 9.3 mM monomer + 0.5 M H_2SO_4 solution at the surface of CNTPE, (A) in the presence of 5.0 mM Triton X-100 and (B) in the absence of the surfactant at $\upsilon = 0.05\,V\,s^{-1}$. The arrows indicate the trends of current during of cyclic voltammetry.

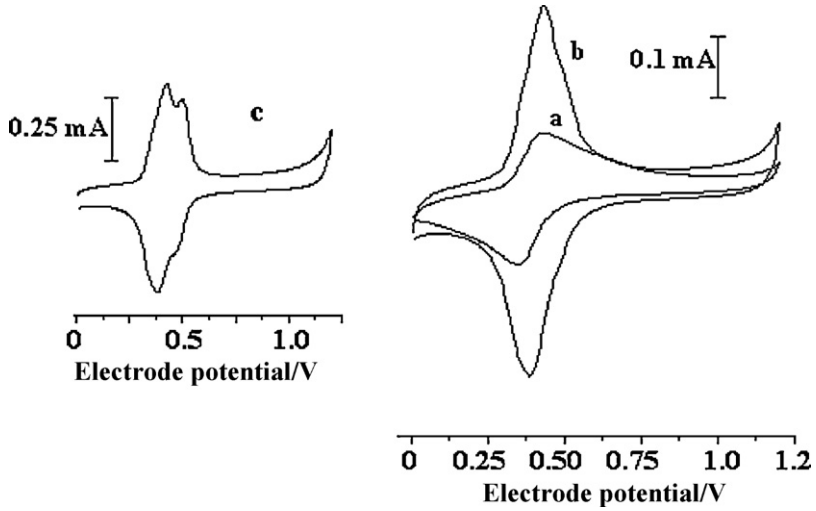

Fig. 2. Cyclic voltammograms of POT/MCNTPE (a) and POT (TX-100)/MCNTPE (b) after potential cycling in 0.5 M H_2SO_4. (c) The first cyclic voltammogram of POT (TX-100)/MCNTPE after immersing in 0.5 M H_2SO_4 solution at $\upsilon = 0.05\,V\,s^{-1}$.

film shows large background current. This is also attributed to the large surface area of porous structure of the film immobilized on the surface of CNTPE. The redox behavior of the films is strongly dependent on the pH of the electrolyte solution. As can be seen in Fig. 2, obtained polymer shows a well-defined redox behavior in acidic supporting electrolyte solution. The response obtained in an alkaline solution (i.e., 0.1 M NaOH) shows a complete loss of electrode activity (figure not shown). However, the films are not degraded under these experimental conditions and their responses are recovered when the electrodes are immersed in an acidic supporting electrolyte solution.

Fig. 3A represents the cyclic voltammograms of POT (TX-100)/MCNTPE in 0.5 M H_2SO_4 solution recorded at different potential sweep rates, υ, in a wide range of 0.005–1.00 $V\,s^{-1}$. Anodic

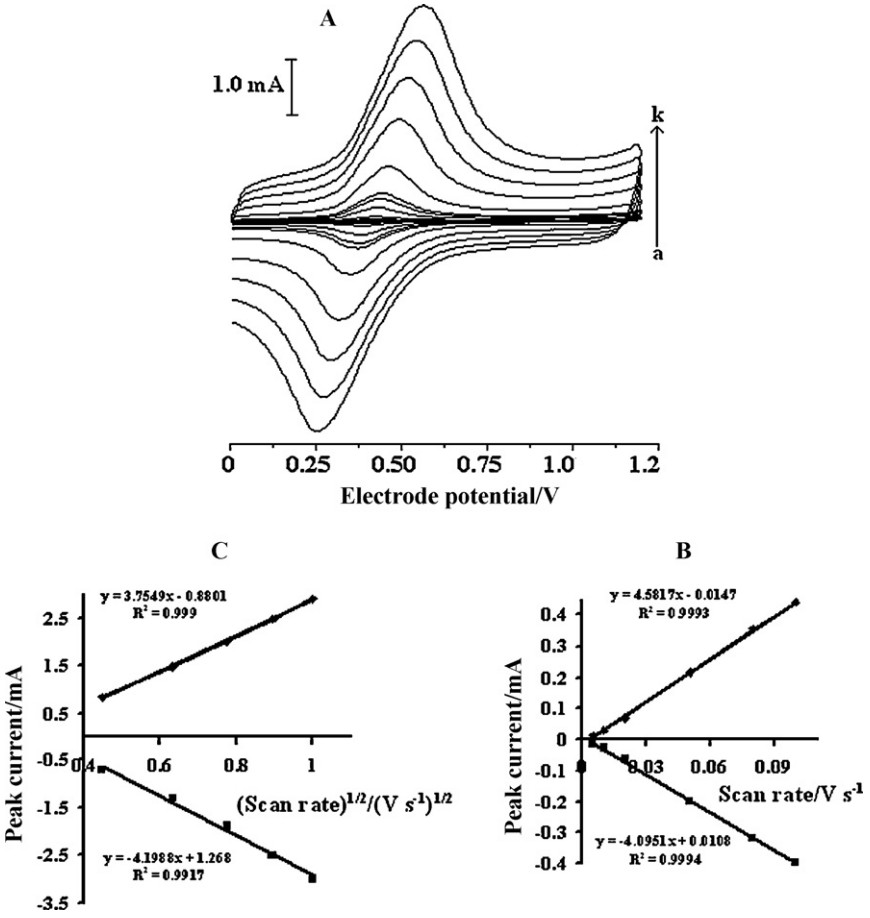

Fig. 3. (A) Cyclic voltammograms of POT (TX-100)/MCNTPE in 0.5 M H_2SO_4 solution at various sweep rates of potential: (a) 0.005, (b) 0.01, (c) 0.02, (d) 0.05, (e) 0.08, (f) 0.10, (g) 0.20, (h) 0.40, (i) 0.60, (j) 0.80 and (k) 1.0 $V\,s^{-1}$. (B) The dependency of peak currents on the υ at lower values (0.005–0.10 $V\,s^{-1}$) and (C) on the $\upsilon^{1/2}$ at higher values ($\upsilon > 0.10\,V\,s^{-1}$).

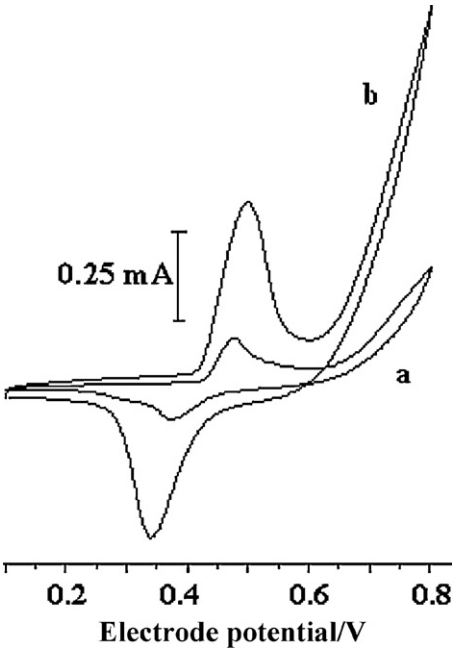

Fig. 4. Cyclic voltammograms of (a) Ni/POT/MCNTPE and (b) Ni/POT (TX-100)/MCNTPE in a 0.1 M NaOH solution after nickel hydroxide formation at scan rate of 0.05 V s^{-1}.

and cathodic peak currents are linearly proportional to υ at low values from 0.005 to 0.080 V s^{-1} (Fig. 3B). This result is attributed to the electrochemical activity of an immobilized redox couple at the surface of electrode. In the higher range of potential sweep rates (0.10–1.0 V s^{-1}; Fig. 3C); the peak currents are linearly proportional to $\upsilon^{1/2}$, showing the dominance of a diffusion-controlled process. This limiting diffusion process may occur for the charge neutralization of the polymer film with ion dopants during its oxidation/reduction process.

3.3. Electrochemical behavior of Ni/POT (TX-100)/MCNTPE

Nickel(II) ions link covalently to the amine groups in the POT (TX-100) backbone creating a structure more stable than that attained by the immersion of bare CNTPE in nickel solutions. After incorporation of Ni^{2+} ions onto the polymer films, polarization behavior is examined in 0.1 M NaOH solution using cyclic voltammetry technique. This technique allows the hydroxide film formation in parallel to inspecting the electrochemical reactivity of the surface. The significant difference between the cyclic voltammogram obtained for immobilized nickel on the POT/MCNTPE (Fig. 4a) and that obtained on the POT (TX-100)/MCNTPE (Fig. 4b) is an increase in area under the curve for the Ni/POT (TX-100)/MCNTPE. This improvement may be resulted from an interaction between the nickel ions and TX-100 presented in the POT films. This porous structure yields larger available area

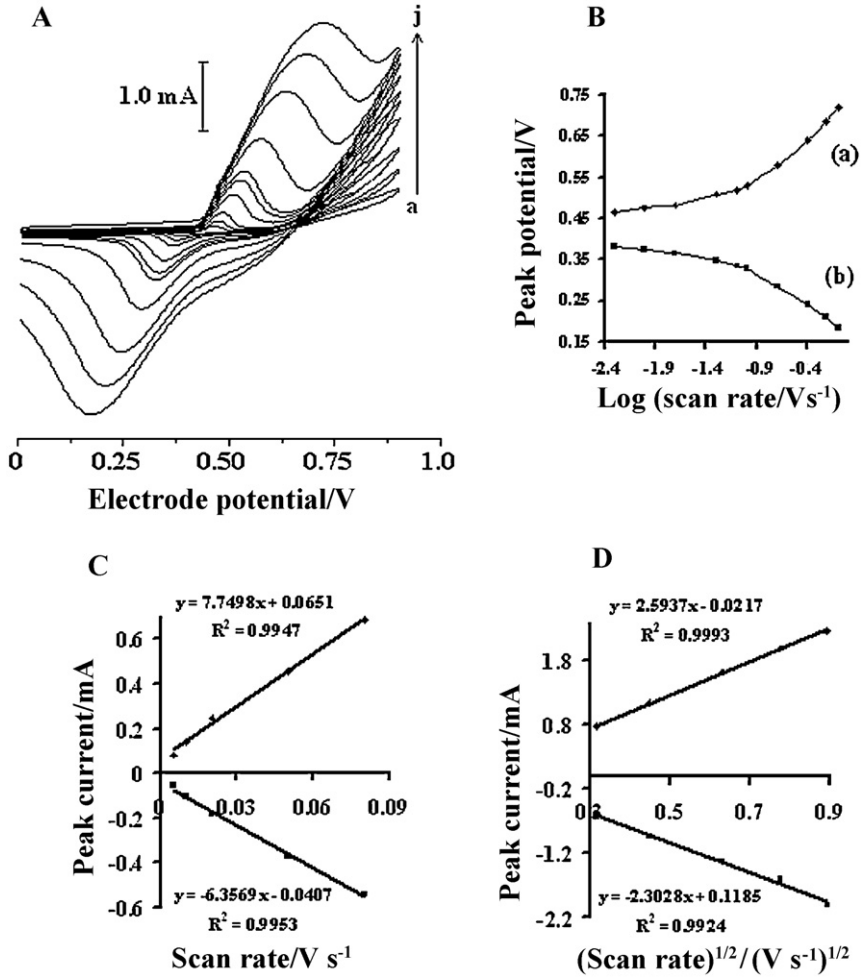

Fig. 5. (A) Cyclic voltammograms of Ni/POT (TX-100)/MCNTPE at various potential scan rates: (a) 0.005, (b) 0.01, (c) 0.02, (d) 0.05, (e) 0.08, (f) 0.10, (g) 0.20, (h) 0.40, (i) 0.60 and (j) 0.80 V s^{-1}. (B) Plot of E_p vs. log υ for cyclic voltammograms depicted in the (A) for anodic peaks (a) and cathodic peaks (b). (C) The dependency of anodic and cathodic peak currents on lower values of υ (0.005–0.08 V s^{-1}) and (D) on $\upsilon^{1/2}$ at higher values of υ (υ > 0.08 V s^{-1}).

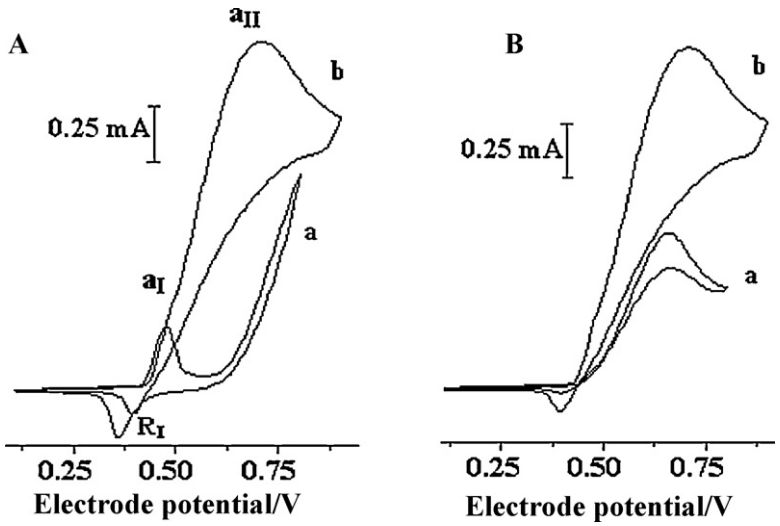

Fig. 6. (A) Electrochemical responses of Ni/POT (TX-100)/MCNTPE in 0.1 M NaOH (a) in the absence and (b) the presence of 0.24 M methanol. (B) Cyclic voltammograms of (a) Ni/POT/MCNTPE and (b) Ni/POT (TX-100)/MCNTPE in 0.1 M NaOH + 0.24 M CH_3OH at $\upsilon = 0.02\,V\,s^{-1}$.

and, in the case of introducing of nickel, with a better dispersion and/or distribution. The redox process of these modified electrodes is expressed as:

$$Ni(OH)_2 + OH^- \rightleftarrows NiOOH + H_2O + e^- \quad (1)$$

Fig. 5A shows the cyclic voltammograms obtained at the surface of Ni/POT (TX-100)/MCNTPE at different scan rates of potential in a wide range of 0.005–0.8 V s^{-1}. A pair of well-defined peaks with a half wave potential of 425 mV appears in the voltammograms, and the peak-to-peak potential separation (at the potential sweep rate of 10 mV s^{-1}) is 98 mV. The peak-to-peak potential separation is deviated from the theoretical value of zero and increases at higher potential sweep rates. This result indicates a limitation in the charge-transfer kinetics arising from chemical interactions between the electrolyte ions and the modifier film, dominated of electrostatic factors, and/or non-equivalent sites present in the film. Laviron derived general expressions for the linear potential sweep voltammetric response in the case of surface-confined electroreactive species at small concentrations [33]. The expressions for peak-to-peak separation of $\Delta E_p > 0.2/n$ V, where n is the number of exchanged electrons, are as follows:

$$E_{pa} = E^0 + A \ln\left[\frac{1-\alpha}{m}\right] \quad (2)$$

$$E_{pc} = E^0 + B \ln\left[\frac{\alpha}{m}\right] \quad (3)$$

$$\text{Log}\, k_s = \alpha \log(1-\alpha) + (1-\alpha)\log\alpha - \log\left(\frac{RT}{nF\upsilon}\right) - \frac{\alpha(1-\alpha)nF\Delta E_p}{2.3RT} \quad (4)$$

where $A = RT/(1-\alpha)nF$, $B = RT/\alpha nF$, $m = (RT/F)(k_s/n\upsilon)$, E_{pa}, E_{pc}, α, k_s and υ are anodic, cathodic peak potentials, anodic electron transfer coefficient, apparent charge transfer rate constant and potential sweep rate, respectively. From these expressions, α can be determined by measuring the variation of the peak potential with respect to the potential sweep rate, and k_s can be determined for electron transfer between the electrode and surface deposited layer by measuring the E_p values. Fig. 5B shows the plot of E_p with respect to the logarithm υ from cyclic voltammograms recorded at potential sweep rates 0.005–0.08 V s^{-1} for anodic (a) and cathodic (b) peaks. It can be observed that the values of E_p are proportional to the logarithm υ at $\upsilon > 0.08\,V\,s^{-1}$ indicated by Laviron. Using the plot and Eqs. (2) and (4), the value of α is determined to be 0.7. In addition, the value of β (cathodic electron transfer coefficient) is determined to be 0.3. These discrepancies suggest that the rate-limiting steps for the reduction and oxidation processes might not be the same [34,35]. Moreover, the mean value of k_s is determined to be 2.86 s^{-1}.

Another point in the voltammograms represented in Fig. 5A is that the anodic and cathodic peak currents are proportional to the υ at low values from 0.005 to 0.08 V s^{-1} (Fig. 5C). This can be attributed to an electrochemical activity of an immobilized redox couple at the surface. From the slope of this line and using [36]:

$$I_p = \frac{n^2F^2\upsilon A\Gamma^*}{4RT} \quad (5)$$

where I_p, A and Γ^* are peak current, electrode surface area and surface coverage of the redox species, respectively, and taking the average of both cathodic and anodic currents, the total surface coverage of the immobilized active substance in the film of about 8.28×10^{-8} mol cm^{-2} is derived. In the higher range of υ ($\upsilon > 0.08$ V s^{-1}, Fig. 5D), the peak currents depend on $\upsilon^{1/2}$, signifying the dominance of a diffusion process as the rate limiting step in the total redox transition of the modifier film. This diffusion process may be due to the charge neutralization of the film during the oxidation/reduction process [37–39].

3.4. Electrocatalytic oxidation of methanol at the Ni/POT (TX-100)/MCNTPE

The electrochemical response of a Ni/POT (TX-100)/MCNTPE in alkaline solution exhibits well-defined anodic and cathodic peaks (Fig. 6A (a)) associated with the Ni(III)/Ni(II) redox couple. Fig. 6A (b) shows the behavior of this modified electrode in the presence of 0.24 M methanol. An increment in the anodic peak current (a_I) followed by the appearance of a new peak (a_{II}) at more positive potential and a decrease in the cathodic peak current and its charge (R_I) during the reverse scan are the main effects observed upon methanol addition to the electrolyte solution. The modifier layer $Ni(OH)_2$ at the electrode surface acts as a catalyst for the oxidation of methanol in 0.1 M NaOH solution. As has been reported in the literature [40–44], this behavior is typical of that expected for mediated oxidation of methanol as follows:

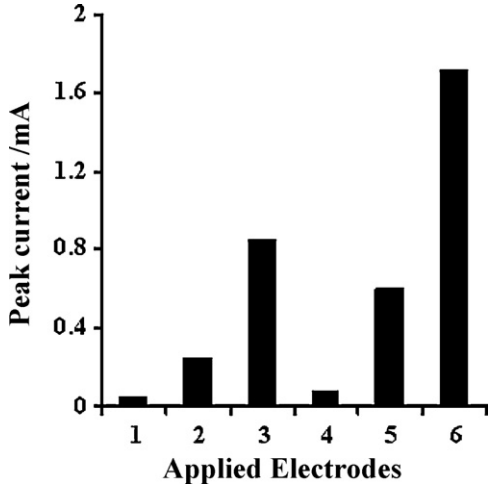

Fig. 7. Histograms of anodic peak currents for, (1) Ni/CPE, (2) Ni/POT/MCPE, (3) Ni/POT (TX-100)/MCPE, (4) Ni/CNTPE, (5) Ni/POT/MCNTPE and (6) Ni/POT (TX-100)/MCNTPE in a solution containing 0.24 M methanol + 0.1 M NaOH at $\upsilon = 0.02\ V\ s^{-1}$.

$$Ni(OH)_2 + OH^- \rightleftharpoons NiOOH + H_2O + e^- \quad E \quad (6)$$

$$NiOOH + CH_3OH \rightarrow Ni(OH)_2 + Product \quad C' \quad (7)$$

The relative decrease of the cathodic peak height in presence of methanol is attributed to the partial consumption of nickel oxyhydroxide species for the methanol oxidation with the formation of nickel hydroxide in accordance of reaction (7). This indicates clearly that the applied modifier in this process participates directly in the electrocatalytic oxidation of methanol.

It is generally agreed that the Ni-based catalysts such as nickel oxides and its complexes in a basic aqueous medium can catalyze methanol oxidation through an overall four electron process for producing formate anion [45]:

$$CH_3OH + 5OH^- \rightarrow HCOO^- + 4H_2O + 4e^- \quad (8)$$

For comparison, the cyclic voltammograms of methanol oxidation at Ni/POT/MCNTPE and Ni/POT (TX-100)/MCNTPE are shown in Fig. 6B. The Ni/POT (TX-100)/MCNTPE yields much higher mass activity (i.e., current normalized per Ni load/A g_{Ni}^{-1}) about (3470 A g_{Ni}^{-1}) than the other electrode (2370 A g_{Ni}^{-1}). The difference between cyclic voltammogram (a) with (b) may be attributed to the large real surface area of the Ni ions in the POT (TX-100) film immobilized on the CNTPE. In addition, the polymeric structure prevents the particle agglomerating and coalescing during accumulation and also stabilizes them on the electrode. These observations can clearly explain the role of the POT (TX-100) film on the enhancement of electrocatalytic oxidation currents of methanol. Indeed, the POT (TX-100) film is a good and proper bed for immobilization of nickel ions. It seems that the main and plausible reason for such an enhancement is the formation of a polymer film backbone at the surface of CNTPE that provides the facile arrival of methanol on $Ni(OH)_2$ catalytic centers.

The anodic currents for methanol electrooxidation under the same conditions at the surface of various electrodes are given in Fig. 7. Methanol does not undergo oxidation prior to the discharge of supporting electrolyte at CPE and CNTPE in potential window (0.1–0.9 V) in 0.1 M NaOH solution, while a small current is observed in the case of the Ni/CPE. Following the dispersion of nickel ions at the POT/MCPE surface, methanol oxidation occurs at this electrode with higher current. This may be attributed to the presence of polymeric film having amine groups which increases

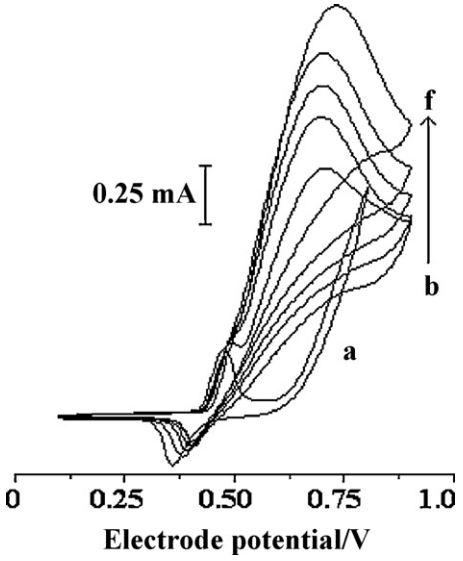

Fig. 8. Current–potential curves of different methanol concentrations: (a) 0.0 M, (b) 0.06 M, (c) 0.12 M, (d) 0.18 M, (e) 0.24 M and (f) 0.3 M at the surface of Ni/POT (TX-100)/MCNTPE at the potential scan rate of $0.02\ V\ s^{-1}$.

the amount of accumulated nickel. Ni/POT (TX-100)/MCPE shows higher catalytic current with respect to the previous electrodes. Also, the application of MWCNTs as incorporated materials into a carbon paste electrode improves the electrochemical signal of methanol oxidation and thus the highest current is obtained at the surface of Ni/POT (TX-100)/MCNTPE.

3.5. The effect of methanol concentration

Fig. 8 shows the effect of methanol concentration on the anodic peak current at Ni/POT (TX-100)/MCNTPE in 0.1 M NaOH. It is clearly observed that as the methanol concentration increases, the peak height increases linearly with methanol concentration up to 0.24 M. It can be assumed that the increase is due to the presence of a diffusion controlled process that appears to play an important role at low methanol concentrations. While the methanol concentration exceeds this limit, the rate of the whole oxidation process seems to be limited by that of the catalytic process in origin and its rate depends on the reaction between methanol and Ni(III) species, which is present in the film.

3.6. Chronoamperometric studies

Double potential step chronoamperometry is employed for the investigation of electrochemical processes at the Ni/POT (TX-100)/MCNTPE surface. Fig. 9A shows the double-step chronoamperograms for the modified electrode by setting the working electrode potential at 0.7 V (first step) and 0.3 V (second step) vs. Ag|AgCl|KCl (3 M) for various concentrations of methanol. In the presence of methanol, the charge value associated with the forward chronoamperometry, Q_a, is greater than that observed for the backward chronoamperometry (Fig. 9B (e′)). Chronoamperometry can also be used for the evaluation of the chemical reaction between the methanol and modified layer (catalytic rate constant, k) according to [36]:

$$\frac{I_C}{I_L} = \pi^{1/2}\lambda^{1/2} = \pi^{1/2}(kc_o t)^{1/2} \quad (9)$$

where I_C and I_L are the currents in the presence and absence of methanol, k is catalytic rate constant; c_o is the bulk concentration of methanol and t is the elapsed time. From the slope of the

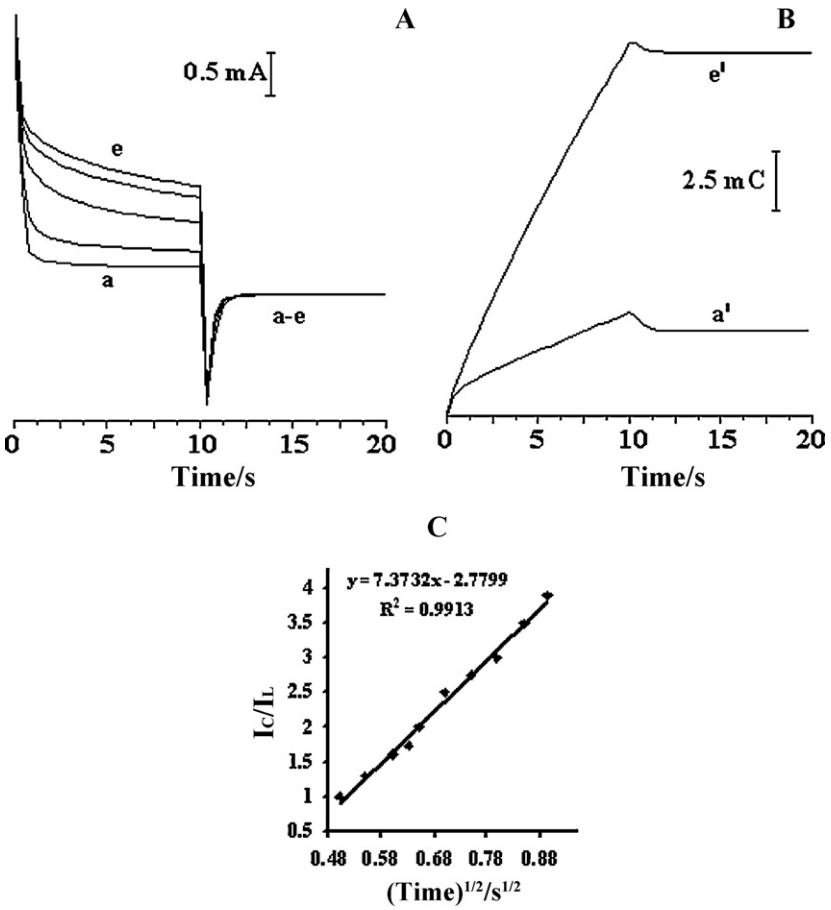

Fig. 9. (A) Chronoamperograms obtained at a Ni/POT (TX-100)/MCNTPE in the absence (a) and the presence of (b) 0.024 M, (c) 0.048 M, (d) 0.072 M and (e) 0.096 M of CH_3OH. (B) The dependency of charge Q (mC) vs. t, derived from the data of chronoamperograms of (a) and (e). (C) The dependency of I_C/I_L on $t^{1/2}$ derived from the data of chronoamperograms of (a) and (e) in the main panel.

Table 1
Comparison of the catalytic rate constant (k, $cm^3\ mol^{-1}\ s^{-1}$) of some Ni-modified electrodes used in electrocatalytic oxidation of methanol.

Electrode	Modifier	Catalytic rate constant	Reference
MWCNTPE	Poly-Ni(II)-quercetin	1.83×10^6	[39]
Glassy carbon	Poly-Ni(II)-curcumin	2.04×10^3	[44]
Ni–Cu alloy	$Ni(OH)_2$	1.98×10^3	[46]
Carbon paste	Ni/POAP	8.67×10^1	[47]
Carbon nanotube paste	Ni/POT (TX-100)	7.40×10^4	This work

I_C/I_L vs. $t^{1/2}$ plot, presented in Fig. 9C, the mean value of k for the concentration range of 0.024–0.12 M of methanol is obtained as $7.40 \times 10^4\ cm^3\ mol^{-1}\ s^{-1}$. This estimated k value is comparable with other k values for similar systems in the literature (see Table 1).

3.7. Long-term stability of Ni/POT (TX-100)/MCNTPE

In the practical view, long-term stability of the electrode is important. The long-term stability of Ni/POT (TX-100)/MCNTPE is examined in 0.1 M NaOH + 0.24 M CH_3OH solutions using cyclic voltammetry method (figure not shown). The anodic peak current decreases gradually with potential cycling. In general, the loss of the catalytic activity with successive scans of potential may result from the consumption of methanol during the scan of potential in cyclic voltammetry. It also perhaps due to poisoning and the structure change of the nickel as a result of the perturbation of the potentials during the scanning in aqueous solutions, especially in the presence of organic compound. Another factor may be due to the diffusion process occurring between surface of the

Table 2
Comparison of the efficiency (in terms of current density) and anodic peak potential (a_{II}) of some Ni-modified electrodes used in electrocatalytic oxidation of methanol in alkaline medium.

Electrode	Modifier	[a] j ($mA\ cm^{-2}$)	υ ($mV\ s^{-1}$)	$E_{p(a_{II})}$ (V)	Reference
Glassy carbon	Ni^{II}-DHS	6.9	20	0.63	[37]
Nickel	NiODMG	15.9	20	0.60	[40]
Glassy carbon	$Ni(OH)_2$	15.4	50	0.58	[41]
Glassy carbon	Poly-(Ni^{II}-tmdbta)	1.5	100	0.61	[42]
Nickel	NiODMG	16.1	20	0.62	[43]
Glassy carbon	Poly-Ni(II)-curcumin	17.2	100	0.77	[44]
Carbon paste	Ni/POAP	3.7	20	0.70	[47]
Carbon	NiHS	25.1	5	0.60	[49]
Carbon paste	Ni/P-1,5-DAN	1.54	10	0.65	[50]
Carbon nanotube paste	Ni/POT (TX-100)	18.5	20	0.70	This work

[a] Current density: $j = I_p(aII)/A$ (A is the geometric surface area of substrate).

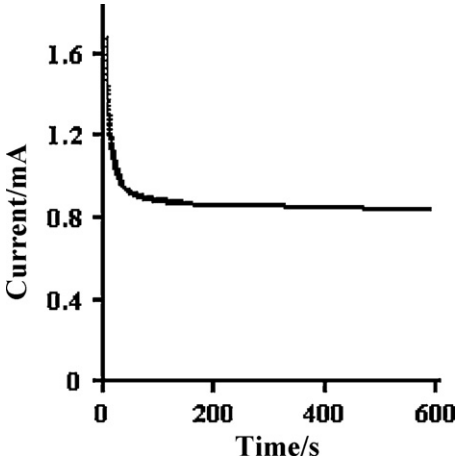

Fig. 10. Current–time transient for methanol oxidation at the surface of Ni/POT (TX-100)/MCNTPE in the presence of 0.24 M methanol in 0.1 M NaOH solution for a period of 600 s. The potential step was 0.75 V.

electrode and the bulk solution. With increasing of scan number, methanol diffuses gradually from the bulk solution to the electrode surface.

It was reported by Jiang and coworkers [48] that the methanol oxidation current on Pt polycrystalline electrode decays rapidly with the time, and the current in *i*–*t* curve is almost zero after 400 s. The rapid current decay has been interpreted as the "self-poisoning" of the adsorbed species derived from the dissociative adsorption of methanol. In this work, for further evaluate the activity and stability of the Ni/POT (TX-100)/MCNTPE, chronoamperogram was recorded for a large time window of our modified electrode in the presence of methanol (Fig. 10). As can be seen, the decrease in current is relatively slow. It is obvious that the Ni/POT (TX-100)/MCNTPE exhibits a good stability toward methanol oxidation. In comparison with some other previous works, it seems clearly that nickel hydroxide in the modified electrode can act as a comparable catalyst in methanol electrooxidation (see Table 2).

4. Conclusion

In this work, a novel poly(*o*-toluidine)/Triton X-100 film was prepared by electropolymerization of OT at the surface of carbon nanotube paste electrode in the presence of TX-100. Addition of TX-100 to the monomer solution leads to an increase in the polymer growth rate. Also, TX-100 in the electrolyte solution may be adsorbed on the electrode and changes the interfacial structure between electrode and electrolyte, which benefits the preparation of poly(*o*-toluidine) with more current density. The electrochemical behavior of POT (TX-100)/MCNTPE shows that, apart from the higher polymerization rate in the presence of TX-100, the resulting polymer has good electrical conductivity, which can be due to the different morphology of poly(*o*-toluidine) in the POT (TX-100)/MCNTPE.

$Ni(OH)_2$ species onto the poly(*o*-toluidine)/Triton X-100 film shows higher catalytic activity towards methanol oxidation than that the other nickel modified electrodes. The value for the catalytic rate constant obtained from the chronoamperometric method indicates that the modified electrode can overcome the kinetic limitation for the methanol oxidation by a catalytic process and can decrease the overpotential for the oxidation reaction of methanol. The stability of the Ni/POT (TX-100)/MCNTPE seems to be acceptable for practical applications.

References

[1] Z.B. Wang, G.P. Yin, P.F. Shi, Carbon 44 (2006) 133–140.
[2] A. Lima, C. Coutanceau, J.-M. Leger, C. Lamy, J. Appl. Electrochem. 31 (2001) 379–386.
[3] D. Pan, J. Chen, W. Tao, L. Nie, S. Yao, Langmuir 22 (2006) 5872–5876.
[4] W. Sugimoto, T. Saida, Y. Takasu, Electrochem. Commun. 8 (2006) 411–415.
[5] E. Antolini, J. Power Sources 170 (2007) 1–12.
[6] H.J. Salavagione, C. Sanchis, E. Morallon, J. Phys. Chem. C 111 (2007) 12454–12460.
[7] F.S. Hoor, C.N. Tharamani, M.F. Ahmed, S.M. Mayanna, J. Power Sources 167 (2007) 18–24.
[8] V. Neburchilor, H. Wang, J. Zhang, Electrochem. Commun. 9 (2007) 1788–1792.
[9] G.-Y. Zhao, C.-L. Xu, D.-J. Guo, H. Li, H.-L. Li, J. Power Sources 162 (2006) 492–496.
[10] J. Prabhuram, T.S. Zhao, Z.X. Liang, R. Chen, Electrochim. Acta 52 (2007) 2649–2656.
[11] B. Habibi, M.H. Pournaghi-Azar, H. Abdolmohammad-Zadeh, H. Razmi, Int. J. Hydrogen Energy 34 (2009) 2880–2892.
[12] K.W. Park, J.H. Choi, K.S. Ahn, V.E. Sung, J. Phys. Chem. B 108 (2004) 5989–5994.
[13] R. Parsons, T.J. Vandernoot, J. Electroanal. Chem. 257 (1988) 9–45.
[14] K. Nishimura, K. Machida, M. Enyo, J. Electroanal. Chem. 251 (1988) 117–125.
[15] N.M. Markovic, T.J. Schmidt, B.N. Grgur, H.A. Gasteiger, R.J. Behw, P.N. Ross, J. Phys. Chem. B 103 (1999) 8568–8577.
[16] R.N. Singh, T. Sharma, A. Singh, E. Anindita, D. Mishra, Int. J. Electrochem. Sci. 2 (2007) 762–777.
[17] H.-C. Yu, K.-Z. Fung, T.-C. Guo, W.-L. Chang, Electrochim. Acta 50 (2004) 811–816.
[18] M. Jafarian, R.B. Moghaddam, M.G. Mahajani, F. Gobal, J. Appl. Electrochem. 36 (2006) 913–918.
[19] M.A.A. Rahim, R.M.A. Hameed, M.W. Khalil, J. Power Sources 134 (2004) 160–169.
[20] M. Jafarian, M.G. Mahajani, H. Heli, F. Gobal, H. Khajehsharifi, M.H. Hamedi, Electrochim. Acta 48 (2003) 3423–3429.
[21] G. Inzelt, M. Pineri, J.W. Schultze, M.A. Vorotyntsev, Electrochim. Acta 45 (2000) 2403–2421.
[22] F. Bensebaa, A.A. Farah, D. Wang, C. Bock, X. Du, J. Kung, Y.L. Page, J. Phys. Chem. B 109 (2005) 15334–15339.
[23] G. Dryhrst, D.L. McAllister, in: P.T. Kissinger, W.R. Heinemann (Eds.), Laboratory Techniques in Electroanalytical Chemistry, Marcel Dekker, New York, 1984, p. 289.
[24] C.M.V.B. Almeida, B.F. Giannetti, Elctrochem. Commun. 4 (2002) 985–988.
[25] A.D.W. Carswell, E.A. O'Rear, B.P. Grady, J. Am. Chem. Soc. 125 (2003) 14793–14800.
[26] J.B. Raoof, M.A. Karimi, S.R. Hosseini, S. Mangelizadeh, J. Electroanal. Chem. 638 (2010) 33–38.
[27] S.K. Dhawan, D.C. Trivedi, J. Appl. Electrochem. 22 (1992) 563–572.
[28] W.S. Huang, B.D. Humphrey, A.G. MacDiarmid, J. Chem. Soc. Faraday Trans. 82 (1986) 385–390.
[29] D.D. Borole, U.R. Kapadi, P.P. Mahulikar, D.G. Hundiwale, Mater. Lett. 58 (2004) 3816–3822.
[30] D.D. Borole, U.R. Kapadi, P.P. Kumbhar, D.G. Hundiwale, Mater. Lett. 56 (2002) 685–691.
[31] J.M. Leger, B. Beden, C. Lamy, Synth. Met. 62 (1994) 9–15.
[32] Z. Cai, J. Lei, W. Liang, V. Menon, C.R. Martin, Chem. Mater. 3 (1990) 960–967.
[33] E. Laviron, J. Electroanal. Chem. 101 (1979) 19–28.
[34] M. Hajjizadeh, A. Jabbari, H. Heli, A.A. Moosavi, A. Shafiee, K. Karimian, Anal. Biochem. 373 (2008) 337–348.
[35] H. Luo, Z. Shi, N. Li, Z. Gu, Q. Zhuang, Anal. Chem. 73 (2001) 915–920.
[36] A.J. Bard, L.R. Faulkner, Electrochemical Methods Fundamentals and Applications, Wiley and Sons, New York, 2001.
[37] M.R. Parra, T. Garca, E. Lorenzo, F. Pariente, Sens. Actuators B 130 (2008) 730–738.
[38] J. Taraszewska, G. Roslonek, J. Electroanal. Chem. 364 (1994) 209–213.
[39] L. Zheng, J.-F. Song, J. Solid State Electrochem. 14 (2010) 43–50.
[40] A.N. Golikand, M. Asgari, M.G. Maragheh, S. Shahrokhian, J. Electroanal. Chem. 588 (2006) 155–160.
[41] A.A. El-Shafei, J. Electroanal. Chem. 471 (1999) 89–95.
[42] S.J. Liu, Electrochim. Acta 49 (2004) 3235–3241.
[43] A.N. Golikand, S. Shahrokhian, M. Asgari, M.G. Maragheh, L. Irannejad, A. Khanchi, J. Power Sources 144 (2005) 21–27.
[44] A. Ciszewski, G. Milczarek, B. Lewandowska, K. Krutowski, Electroanalysis 15 (2003) 518–523.
[45] W.S. Cardoso, V.L.N. Dias, W.M. Costa, I.A. Rodrigues, E.P. Marques, A.G. Sousa, J. Boaventura, C.W.B. Bezerra, Ch. Song, H. Liu, J. Zhang, A.L.B. Marques, J. Appl. Electrochem. 39 (2009) 55–64.
[46] M. Jafarian, R.B. Moghhaddam, M.G. Mahjani, F. Gobal, J. Appl. Electrochem. 36 (2006) 913–918.
[47] R. Ojani, J.B. Raoof, S. Fathi, J. Solid State Electrochem. 13 (2009) 927–934.
[48] Z.F. Chen, Y.X. Jiang, Y. Wang, J.M. Xu, L.Y. Jin, S.G. Sun, J. Solid State Electrochem. 9 (2005) 363–370.
[49] C. Xu, Y. Hu, J. Rong, S.P. Jiany, Y. Liu, Electrochem. Commun. 9 (2007) 2009–2012.
[50] R. Ojani, J.B. Raoof, S.R. Hosseini, Electrochim. Acta 53 (2008) 2402–2407.